J. Fluid Mech. (2011), *vol.* 687, *pp.* 341–359.
doi:10.1017/jfm.2011.357

Clusters in dense-inertial granular flows

Charles S. Campbell†

Department of Aerospace and Mechanical Engineering, University of Southern California, Los Angeles, CA 90089-1453, USA

(Received 9 December 2010; revised 26 May 2011; accepted 25 August 2011; first published online 13 October 2011)

In the dense-inertial regime of granular flow, the stresses scale inertially, but the flow is dominated by clusters of particles. This paper describes observations of cluster development in this regime. Clusters were seen to form for both elastic and inelastic reasons: elastic when the shear rate pushes the particles together faster than the contacts can elastically disperse them, and inelastic as large energy dissipation leads to cluster formation. Furthermore, large particle surface friction leads to cluster formation both for structural reasons, because it generates stronger clusters, and for energetic reasons, as friction dissipates energy. However, the most intriguing result of this work is that clusters appear to have little effect on the rheology of the dense inertial regime, which suggests that one can model the dense inertial regime with entirely collisional hard sphere models, and not have to worry about the complexities of modelling clusters. But at the same time it presents a physical puzzle, as one would normally expect the rheology to be strongly dependent on microstructural features such as clusters, particularly as they present an elastic pathway for internal momentum transport. There is no completely satisfying explanation for why the clusters can be ignored, but two possibilities suggest themselves. Because the clusters are short-lived, it is possible that they do not survive long enough to make a significant contribution to the momentum transport. And it is also possible for the granular temperature that governs transport between clusters to act as a rate-limiting bottleneck that is in overall control of the momentum transport rate.

Key words: granular media, multiphase and particle-laden flows

1. Introduction

Dense-inertial flow describes a regime of granular flow in which globally the material behaves inertially, but the particles exist not as individuals but in short-lived clusters. (This regime was called the 'inertial non-collisional' regime by Campbell (2002), a name that is more accurate than 'dense-inertial' but more awkward.) It is a subregime of the inertial regime of granular flow. Broadly, granular flows can be divided into elastic flows, which are dominated by force chains, and inertial flows, which are not. The stresses in an elastic flow naturally scale with the interparticle stiffness k as $\tau d/k$, where d is the particle diameter. Inertial flows demonstrate Bagnold scaling, $\tau \sim \rho d^2\gamma^2$, where ρ is the particle density and γ is the shear rate (Bagnold 1954). The elastic regime can be further subdivided into the elastic-quasistatic subregime, in which the stresses are independent of shear rate, and the

† Email address for correspondence: campbell@usc.edu

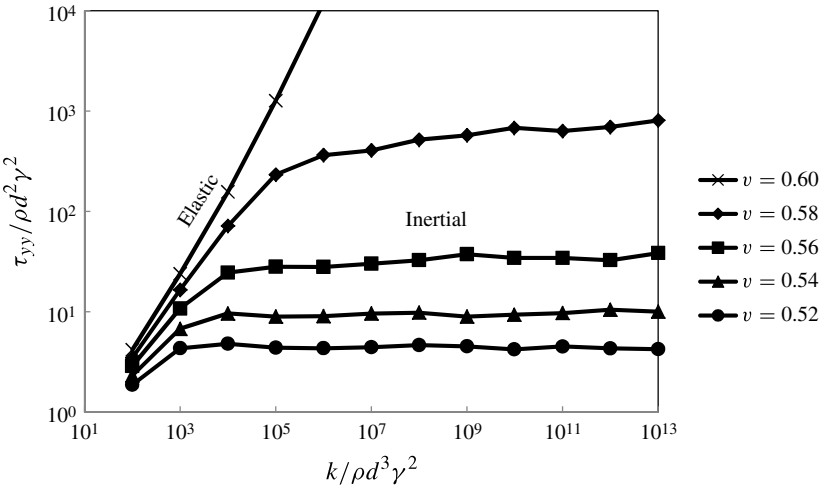

FIGURE 1. Inertially scaled yy stress, $\tau_{yy}/\rho d^2\gamma^2$, as a function of the parameter $k/\rho d^3\gamma^2$. One can clearly divide the flow into the elastic zones, which should plot with a slope near one, and the inertial zones where the scaled stress is nearly constant. Here $\epsilon = 0.7$, $\mu = 0.5$.

elastic-inertial subregime, where the stresses increase linearly with the shear rate above the quasistatic baseline. (There is no difference in the underlying physics of the two subregimes, only that inertia effects are negligible in the elastic-quasistatic regime and become noticeable in the elastic-inertial regime.) Likewise the inertial regimes can be divided into the dense-inertial, dominated by clusters, and the inertial-collisional regime, in which the particles interact collisionally.

Figure 1 shows the inertially scaled τ_{yy} stress as a function of $k^* = k/\rho d^3\gamma^2$ from a simple shear flow. (In this paper, x represents the main flow direction, y is the direction of the velocity gradient, and z is the out-of-shear plane coordinate.) This is similar to a plot in Campbell (2002), but is taken from simulations performed for this paper and extends the Campbell (2002) data to much larger values of k^*. It is easy to differentiate the elastic behaviour, with a slope near 1, and the constant inertial region. (Note that $\nu = 0.58$ is a transitional concentration and shows a slight increase in $\tau_{yy}/\rho d^2\gamma^2$ with k^*. This can be understood by examining time traces of the instantaneous stress that show that force chains sporadically form at $\nu = 0.58$, even at the largest values of k^* studied in this paper. Such a plot for the data in figure 1 can be found in the supplementary material for this paper, available at journals.cambridge.org/flm.) The inertial regions where $\tau_{yy}/\rho d^2\gamma^2$ encompass both the dense-inertial and inertial-collisional regimes. (A referee requested that the various stress ratios, τ_{xy}/τ_{yy}, τ_{yy}/τ_{xx} and τ_{zz}/τ_{xx}, be included in the paper: these can be found in the Appendix.)

Campbell (2002) found that the dense-inertial regime exists at large particle concentrations (for uniformly sized spheres, at a solid fractions ν of 0.52–0.58) and at moderate values of k^*, that is, towards the left side of the inertial region in the curves in figure 1. Campbell (2002) detected that regime by measuring the average contact time, t_c, of the particles relative to the binary collision time, T_{bc}. In the systems studied, the binary collision time is fixed, and the only way for contacts to exist longer than a binary contact time is if at least one of the particles involved interacts with a third particle before the contact breaks. In the dense-inertial regime, the average contact lasted of the order of tens of binary contact times. On one hand this indicates

significant simultaneous multiparticle contacts, and thus the existence of clusters of particles. But on the other hand, it indicates that the clusters are very short-lived, with lives of the order of 10 T_{bc}, and are thus very dynamic structures.

In inertial regimes, the stresses are independent of the stiffness k. In that case one finds for a given material that any component of stress, $\tau = f(\nu, \rho, d, \gamma)$, dictating by dimensional analysis that it must have the Bagnold scaling $\tau = f(\nu)\rho d^2\gamma^2$. This in turn dictates that the apparent friction coefficient τ_{xy}/τ_{yy} (or for that matter any other ratio of stresses) can only be a function of the solid concentration ν. Unfortunately the functional dependence $f(\nu)$ must ultimately be determined empirically. But recently (Midi 2004; da Cruz *et al.* 2005; Jop, Forterre & Pouliquen 2006; Forterre & Pouliquen 2006; Pouliquen *et al.* 2006) it has been popular to invert this process. They define a dimensionless 'inertial number' $I = \gamma\sqrt{\rho/P}$, where the pressure P is one-third the trace of the stress tensor. Thus one can write that $\nu = f(I)$, and consequently one can create a rheology where one writes $\tau = f(I)\rho d^2\gamma^2$ and $\tau_{xy}/\tau_{yy} = f(I)$. The two stated advantages to rewriting Bagnold's rheology in this form are that the concentration ν is difficult to measure and also that the stresses are very sensitive to ν when the flow is dense, magnifying any errors in its measurement. In addition one can bypass the need for something akin to an equation of state to determine the concentration ν. Also, it is assumed that as I goes to zero the system goes to the low-stress critical state (the portion of the critical state curve where particle compressibility is unimportant – see Campbell 2005), although that assumption introduces error, as it ignores the intervening elastic-inertial regime (as again was shown in Campbell 2005). However, such a rheological model is only useful if one knows the pressure P, otherwise one has an awkward rheology in which the stress is a function of itself (for example, it would be difficult to apply the models to the controlled volume flows studied in this paper where the pressure is determined by flow conditions and cannot be *a priori* known). And therein lies the rub, as one can never really know the pressure P *a priori* in a flowing granular material since the normal stresses are anisotropic. Typically, when these models are applied, one substitutes one stress component for the pressure P – usually the hydrostatic stress component, although, technically, one needs to know the solid fraction to compute the hydrostatic stress. If, as in this paper, one considers roughly uni-directional flows such as simple-shear, chutes or landslides, then one typically has some knowledge of the τ_{yy} component, as it must balance gravity or support a force applied at a boundary; but one has little knowledge of the τ_{xx} and τ_{zz} stresses, which are self-equilibrated, and thus no direct knowledge of the actual pressure. Now many of these models were based on two-dimensional disc simulations, where reportedly τ_{xx} and τ_{yy} are within a few per cent of each other. But the normal stress differences are much more significant for three-dimensional flows of spheres. For example, in the studies performed for this paper, τ_{xx} and τ_{yy} can differ by nearly 10 %, but τ_{zz} and τ_{xx} can differ by close to 30 % and the degree of anisotropy depends largely on concentration and material properties. (See the Appendix for stress ratio plots for the data shown in figure 1. See also the supplementary information for normal stress ratios for different material parameters.) And one cannot base a rheology on a single component of stress such as τ_{yy} in an anisotropic system, as a simple axis rotation will change your 'pressure' and thus your answer. Thus there are systemic errors at the core of these rheological models. Finally, if there are deep flows with sidewalls present, the walls can frictionally support the hydrostatic overburden in a manner that cannot be *a priori* predicted (Janssen 1895), and one will not be able to determine the τ_{yy} stress even with full knowledge of the solid concentration distribution: additional information such as the Janssen coefficients

would be required to determine the pressure. This precludes, for example, the use of these models for hoppers, still the most industrially relevant, unsolved problem in granular flow. (For the record, Jop *et al.* 2006 modelled a chute with sidewalls, but the depth of the flowing region was only $\sim$21 % of the wall separation, so Janssen would have little effect.) So while measuring the solid fraction is difficult, it can in principle be done non-intrusively. (For example, there is a long history of using MRI in granular flows, starting with Nakagawa *et al.* 1993 and many other tomographic methods are possible.) At the same time, it is hard to imagine any non-intrusive way of measuring the three independent normal stresses required to accurately determine the pressure. Thus, in the end, inertial number models are applicable to unbounded or loosely bounded flows such as landslides or shallow chute flows, and even then one must accept the systemic errors in their construction.

For the purpose of this paper, a cluster is defined as a network of particles through which, at any instant, one can move between any two member particles by following a path across interparticle contacts. Clusters have been studied in other ways, for example, Lois, Lemaitre & Carlson (2007*a*,*b*) tried to examine the effects of clustering through force correlations, although their approximate simulation method does not handle elastic contacts between particles and thus precludes the type of clusters seen in this paper. But here we just consider them to be a network of contacts without worrying about how those contacts are loaded. These are not to be confused with the inelastic clusters that form at small particle concentrations, such as those first observed by Hopkins & Louge (1991), as those clusters are simply regions of large particle concentration and the particles are often not in contact (although, as we shall see, the inelasticity of the contacts also plays a role in the formation of dense-inertial clusters). To avoid confusion, Hopkins & Louge clusters will henceforth be referred to as 'assemblies'.

Clusters form when $k^* = k/(\rho d^3\gamma^2)$ is small, implying either a small stiffness k or a large shear rate γ (and if k^* is small enough, the clusters may form into force chains). At large k^*, large stiffness k or small shear rate γ, particles interact mostly by binary collisions. Now one expects that the formation of clusters will have a profound impact on the rheology of the system. In particular, within a cluster, momentum can travel elastically through the deformation of the elastic contacts. Free particles transmit momentum through collision and must cross the interparticle separation before they can pass on their momentum by collisions, but particles in a cluster need only move the small distance required to elastically deform the contact. Thus one expects that momentum will be transported much more quickly and efficiently through the cluster than between clusters or between free particles, and cluster formation will have a strong effect on the overall rheology. But, as shall be shown, that is not the case.

2. Computer simulation

This study was performed using a standard soft-particle DEM simulation of the type originally developed by Cundall & Strack (1979). (See Campbell 2006*b* for a discussion of granular simulation methods.) To form a nearly perfect shear flow, the particles are confined in a control volume bounded by Lees–Edwards boundary conditions (Lees & Edwards 1972). In this scheme, a central control volume is surrounded by periodic images of itself in all directions, $\pm x$, $\pm y$ and $\pm z$. The periodic images above and below in the y-direction are set in motion relative to the central control volume to induce a shear rate γ, with the mean velocity in the x-direction and vorticity pointing in the z-direction. This simulates an infinite shear flow with

no boundaries to distort the flow field. The contact model mirrors that of Cundall & Strack (1979) using a linear spring with stiffness, k coupled with a dashpot with associated constant D in the normal direction. Such a configuration corresponds to a unique coefficient of restitution for binary collisions, ϵ, which Campbell (2002) has shown to properly scale the dissipation in the problem. In the tangential direction a second spring with stiffness k (using the same spring constant in the normal and tangential directions allows k to be a unique scale of the simulation) is coupled with a frictional slider with associated coefficient μ. The basic simulation is identical to that used by Campbell (2002) and the reader is directed there for more information.

The unique part of this simulation is a cluster detection algorithm. This is difficult to implement for Lees–Edwards boundaries as a cluster may cross the periodic boundaries of the simulation and re-enter the control volume at another location. It is also possible for a cluster to wrap around and connect with itself. In such a case the cluster is, in effect, infinitely long, as it crosses all the periodic images extending out to infinity. Such infinite clusters turn out to be quite common at the concentrations studied here and, as shall be shown, are true percolations that are independent of control volume size, at least for control volumes larger than $20 \times 20 \times 20$ particles. In effect they are nascent force chains. Campbell (2003) shows that unloaded force chains are unstable, so that in effect force chains can only practically end at a boundary that applies a load to the chain; as a Lees–Edwards configuration effectively has no boundaries, this requires that a stable force chain must be infinitely long and close upon itself. However, the infinite clusters that form here are unstable, despite their length, probably because they do not have enough support from surrounding particles to keep the clusters from buckling.

The cluster detection algorithm is largely a problem of bookkeeping. All the members of a cluster are stored in linked lists. Each particle is associated by a pointer with its cluster. The process begins with particle one. All the particles with which it is in contact are designated as members of its cluster, and so is every particle with which those neighbours are in contact. In this way a cluster is built up. Sometimes a contact will be found with a particle that already inhabits another cluster; then the two clusters are actually one and are merged together. When a contact occurs across a periodic boundary, the information is stored that the new particle is in a different periodic image from the first particle identified in the cluster. In this way a cluster can cross many periodic images as it is built up. In doing so, it is possible for the cluster to encounter a particle that is already a member of the cluster, but in a different periodic image. In that case the cluster has closed on itself and is considered infinitely long.

3. Results

Figure 2 shows some pictures of large clusters taken from a simulation at a solid fraction $\nu = 0.54$ and $k/\rho d^3\gamma^2 = 10^5$, $\epsilon = 0.7, \mu = 0.5$. These pictures show only the particles in a single cluster, and all other particles have been removed from the picture. Note that these clusters cross the periodic boundaries of the control volume, sometimes several times. For visualization purposes, they have been unwrapped so that they may be viewed as if the periodic boundaries do not exist. However, each particle appears only once in each picture, even if the cluster is infinite. If the cluster were infinite, then each particle actually appears infinitely many times in the cluster, but by limiting each particle to only a single appearance, the cluster appears comprehensible although finite. But figure 2 does indicate the wide variety of cluster shapes that can

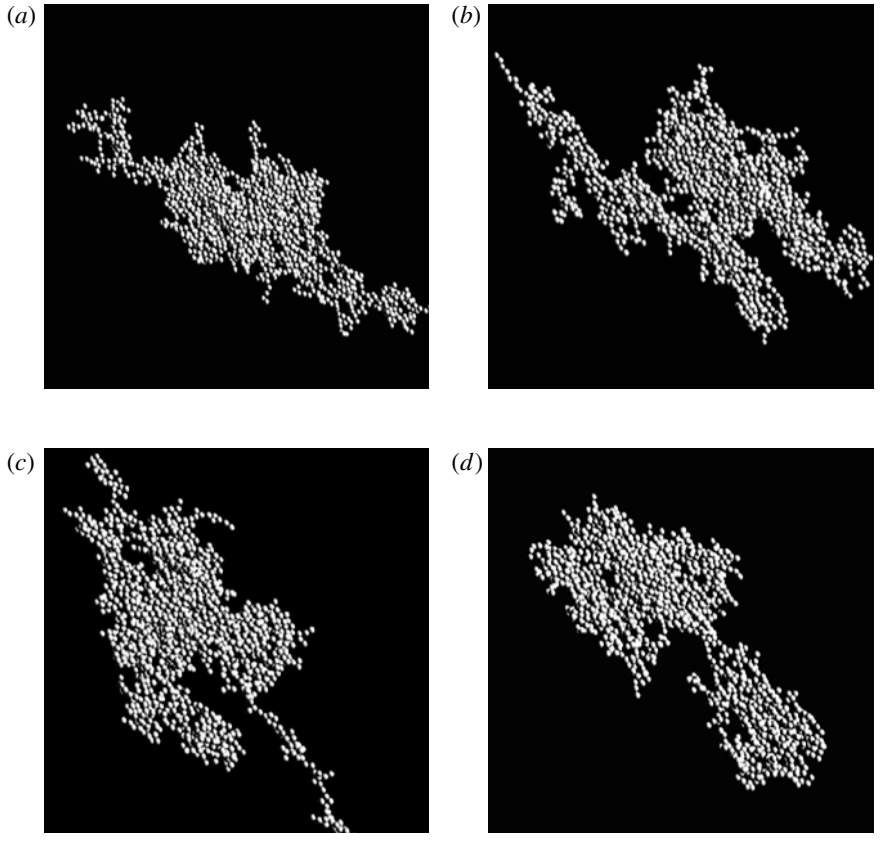

FIGURE 2. Some snapshots of a cluster within a shear flow at $\nu = 0.54$ and $k/\rho d^3\gamma^2 = 10^5$. The cluster has been unwrapped where it crosses periodic boundaries to show how it would look in a larger setting. All other particles have been removed from the image. This visualization was made using *Particlevis*, (Wassgren & Sarkar 2007).

appear within the simulations. However, these clusters are very short-lived. As each contact lasts for only a few binary contact times, and clusters may contain thousands of simulated particles, the clusters noticeably change over a simulation time step. As such they are extremely dynamic structures. Videos of the clusters in action have been uploaded as supplementary material to this paper. Those videos show the progression of a single 'cluster', although making the video entailed identifying a single 'cluster' as it evolves from time step to time step, gathering and shedding large groups of particles. For the purpose of the video, all the clusters in the simulation are assessed at each time step, and the cluster in a subsequent time step is chosen to be the cluster with the most particles in common with the cluster at the previous time step. The four pictures shown in figure 2 are taken from one of the videos, and from that point of view represent the evolution of a single cluster.

Figure 3 shows the probability of a cluster containing N particles. These were all taken from 1000-particle simulations, so the maximum value for N is 1000. On the other side, the smallest 'cluster' size is two, indicating a binary or collisional contact. Naturally there will always be more binary clusters than large clusters, as obviously a thousand particle systems can only accommodate a single 700-particle cluster but at

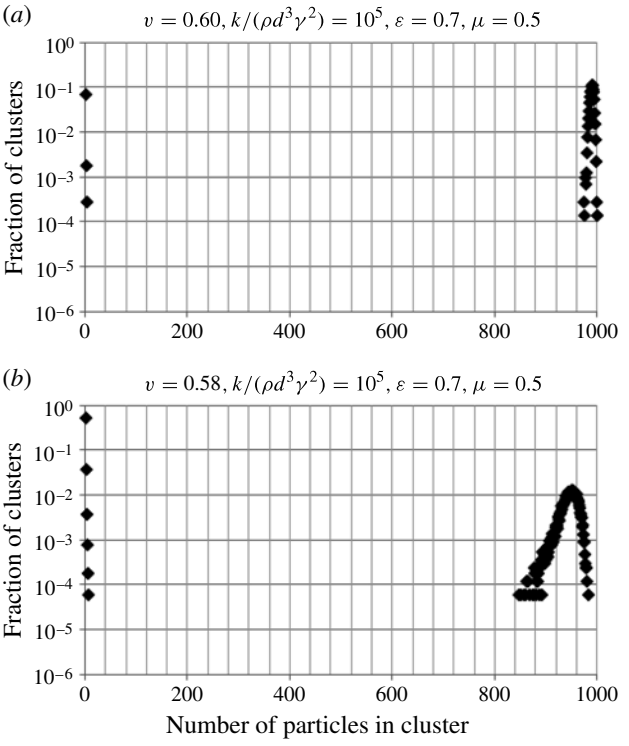

FIGURE 3. For caption see next page.

the same time more than a hundred binary clusters. Thus the probability of finding a large cluster is much smaller than the probability of finding a binary cluster, but while the probability of a large cluster is small, such clusters contain the majority of the particles in the simulation and thus are still most important in the internal force transmission. Many of the figures are divided into two peaks, one at the left side of the graph with a maximum for binary clusters, and the other for infinite clusters. Figure 4 shows the individual peaks in detail. The hump at large particle numbers represents infinite clusters and the small number peak represents binary and finite clusters. Remember that to make an infinite cluster only requires the cluster to close on itself through the periodic boundaries of the system, so that in a $10 \times 10 \times 10$ system, it is possible to generate an infinite cluster with as few as 10 particles. Thus it is not strange to see infinite clusters with a wide range of particle numbers. (Most of the data in this paper are taken from much larger simulations, but 1000-particle simulations are shown here, as the larger the simulation the larger the space between the peaks, making it hard to discern the finite peak. As will be shown, there is little quantitative difference between these 1000-particle and larger simulations.)

With that in mind, it is easier to understand figure 3. Figure 3(*a*) shows a purely elastic case, $\nu = 0.60$, in which the particles are locked in force chains. In that case the chains appear as infinite clusters consisting of nearly every particle in the simulation. The dense-inertial regime enters at $\nu = 0.58$ with a broadening of both the infinite cluster and finite cluster peaks. The peaks merge at $\nu = 0.54$ and the infinite cluster peak has entirely disappeared as a separate entity by $\nu = 0.52$; however, even without a distinct peak, infinite clusters were still observed during the simulation down

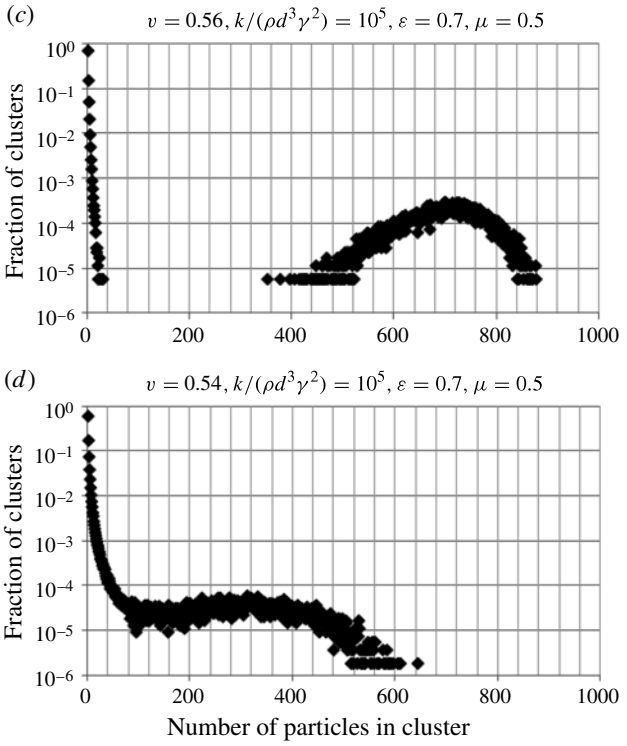

FIGURE 3. For caption see next page.

to $\nu = 0.50$. The only case without infinite clusters is $\nu = 0.45$, which is rheologically a purely collisional flow; but even there, clusters of up to 11 particles were observed during the course of the simulation.

It is convenient to divide the clusters into three categories: binary clusters (indicating collisional interactions), finite but non-binary clusters, and infinite clusters. As this paper concerns rheology, a rheological quantity will be used to evaluate the effects of clusters. Figure 5 shows the fraction of τ_{yy} stress which is supported by clusters of each type for a variety of solid concentrations. For small $k^* = k/\rho d^3\gamma^2$ the stress is entirely supported by infinite clusters. This is interesting because, comparing figure 5(*b*) to the corresponding figure 3(*c*), only ~40–90 % of the particles (with a peak at 70 %) inhabit infinite clusters, yet they support 100 % of the stress, thus demonstrating the importance of clusters in determining the overall rheology. For larger k^* infinite clusters decrease in importance. There is an intermediate range where finite clusters are important. Then, at large k^*, collisions (i.e. binary clusters) dominate the rheology. The dependence on k^* can be understood from the various interpretations of the parameter in Campbell (2002, 2005). One of those interpretations characterizes k^* as a flow time scale (the shear rate $1/\gamma$) divided by an elastic time scale, such as the binary collision time T_{bc}, the time for elastic forces to break a contact. Thus, at small k^*, the particles are being pushed together by the shear rate relatively fast compared to the time that elastic forces break them apart, making it easier for clusters to form. But at large k^* the opposite is true, and elastic forces break the clusters before they can form. Thus infinite clusters dominate at small k^* and binary collisions dominate at large k^*.

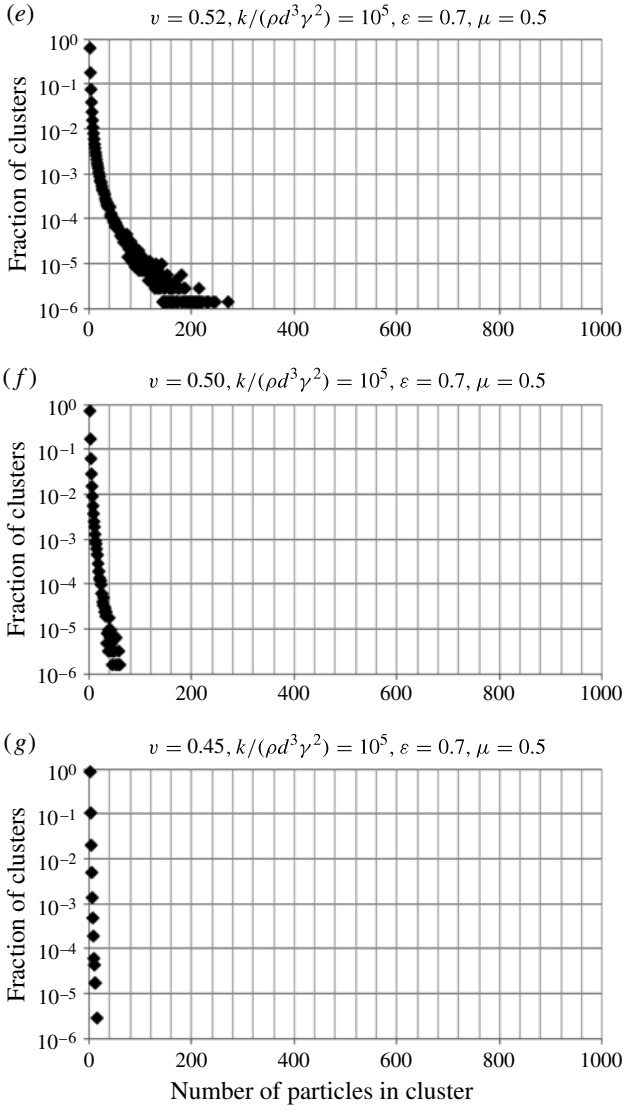

FIGURE 3. The fraction of clusters consisting of N particles. Panel (a) shows a purely elastic flow while (g) is rheologically purely collisional (although clusters of up to 12 particles were observed during the course of the simulation).

At this stage, tests were performed on the effect of control volume size. One might expect infinite clusters to form more readily in smaller control volumes, but the effect is at best weak. One of these tests is shown in figure 5(b), which compares the results from simulations sized $10\times10\times10$ particle spacings (1000 particles) up to $25\times25\times25$ particle spacings (15 625 particles). All the control volume sizes have very similar results, but the infinite/finite cluster transition moves slightly for simulations smaller than $20 \times 20 \times 20$ particles. As a result, $20 \times 20 \times 20$ simulations are used for the rest of the data presented here. (Size tests were performed for all four concentrations shown in figure 5. Only the $\nu = 0.56$ case is shown, both because all the extra lines tend to confuse the graphs and because $\nu = 0.56$ will be the benchmark concentration

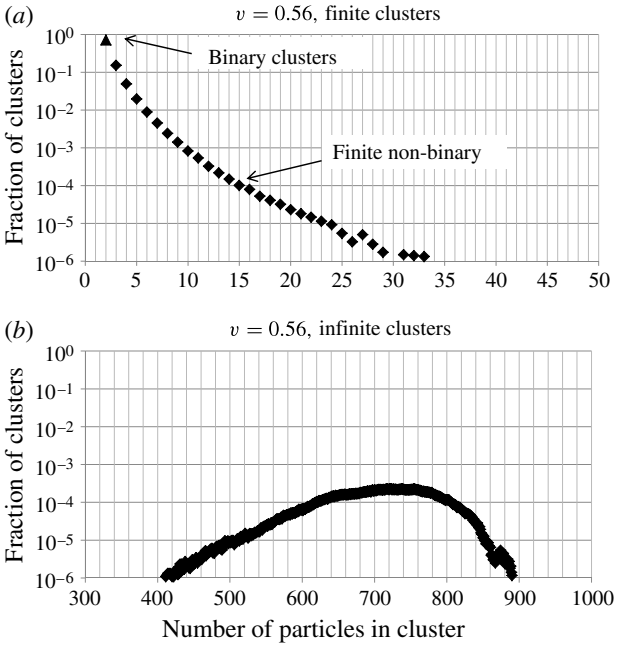

FIGURE 4. The division of the data in figure 3(*c*) into (*a*) binary and finite clusters and (*b*) infinite clusters.

used for the following figures.) These results indicate that the infinite clusters are true percolations and not an effect of control volume size. But note that the small effect observed is the opposite of what one would expect. One would assume that infinite clusters would form more readily for smaller control volumes, but these data indicate the opposite, as decreasing the control volume size moves the infinite/finite transition to the left, indicating that finite, not infinite, clusters appear more readily in smaller systems. Also note that the finite/binary transition is independent of control volume size.

Naturally one expects clusters to be more important at the larger solid concentrations, and from that point of view, figure 5 must come as no surprise. Increasing the concentration ν shifts the infinite/finite and finite/binary transitions towards larger values of $k^* = k/\rho d^3\gamma^2$. The most interesting part of these data is the behaviour of the finite non-binary clusters, which grow in both importance and range in k^* at the smaller concentrations.

Figure 6 shows the effect of the coefficient of restitution ϵ. As can be seen, ϵ has a strong effect and clusters form more readily when there is large dissipation, (when ϵ is small). On one hand these results are not surprising, as in the inertial regimes, where the system is no longer dependent on the interparticle stiffness, k, ϵ is the dominant particle property as it governs the collisional dissipation rate. Thus, in a purely collisional flow at fixed shear rate, ϵ is the largest factor in determining the magnitude of the granular temperature and thus the internal transport rates. But when it comes to cluster formation, both ϵ and k^* affect cluster formation, suggesting a combination of elastic and inelastic effects. (In addition, decreasing the coefficient of restitution lengthens the collision time and slows the rate at which clusters break apart, and thus affect cluster formation in a manner similar to reducing k^*. But that effect

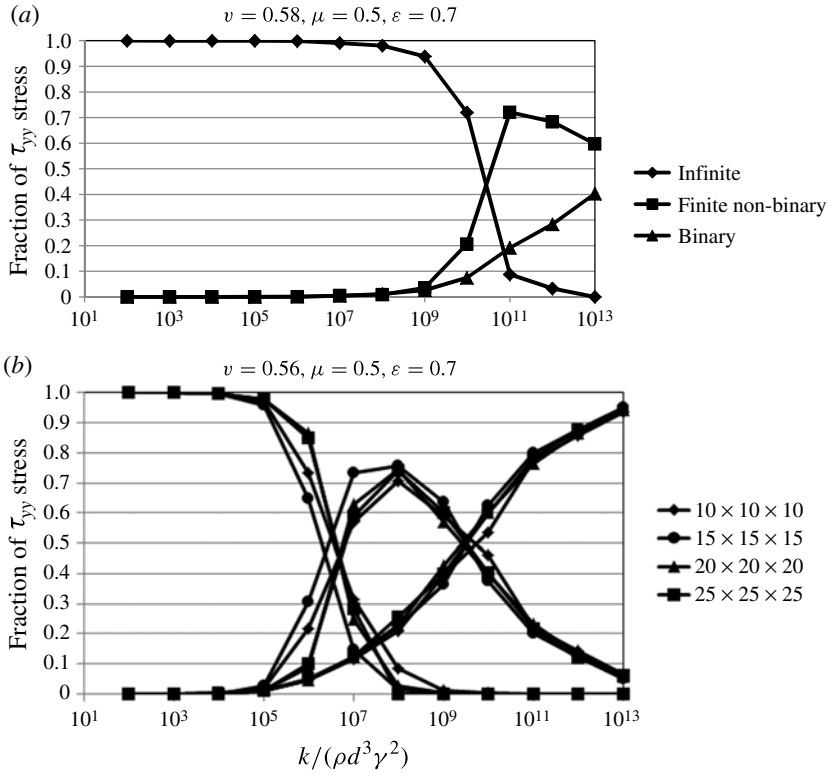

FIGURE 5. For caption see next page.

is probably small, as even decreasing ϵ to 0.1 only increases the binary contact time by $\sim$10 % relative to $\epsilon = 1.0$.) Note that changing ϵ moves both the infinite/finite and finite/binary transitions by a large amount, which suggests that increasing the particle energy by decreasing the dissipation breaks up clusters, whether they be infinite or finite.

One has to wonder whether the effect of ϵ is the same as the collapse physics that led to the inelastic assemblies, such as those first observed at relatively small concentrations by Hopkins & Louge (1991). Indeed, the effect seems much the same. They also saw that the smaller ϵ, the larger the assemblies. Furthermore, they found that the larger the control volume, the larger the assemblies, which might possibly be related to the slight movement of the infinite/finite transition with control volume size in figure 5(*b*). But the physics are somewhat different. Remember that Hopkins & Louge assemblies are regions of higher concentration, and their particles are generally not in contact. It is a density instability, and at the high concentrations studied here, there is simply no room for a density instability to form. They see larger assemblies for larger control volumes simply because there is more room for them to grow. In contrast, the infinite/finite cluster transition is a transition in interparticle connectivity, not concentration and is relatively insensitive to control volume size. In addition, the Hopkins & Louge assemblies affect the stresses, but as shall be seen, these clusters do not.

Figure 7 shows the effect of surface friction μ. Increasing μ shifts both the infinite/finite and finite/binary transitions to the right. Friction plays a dual role in

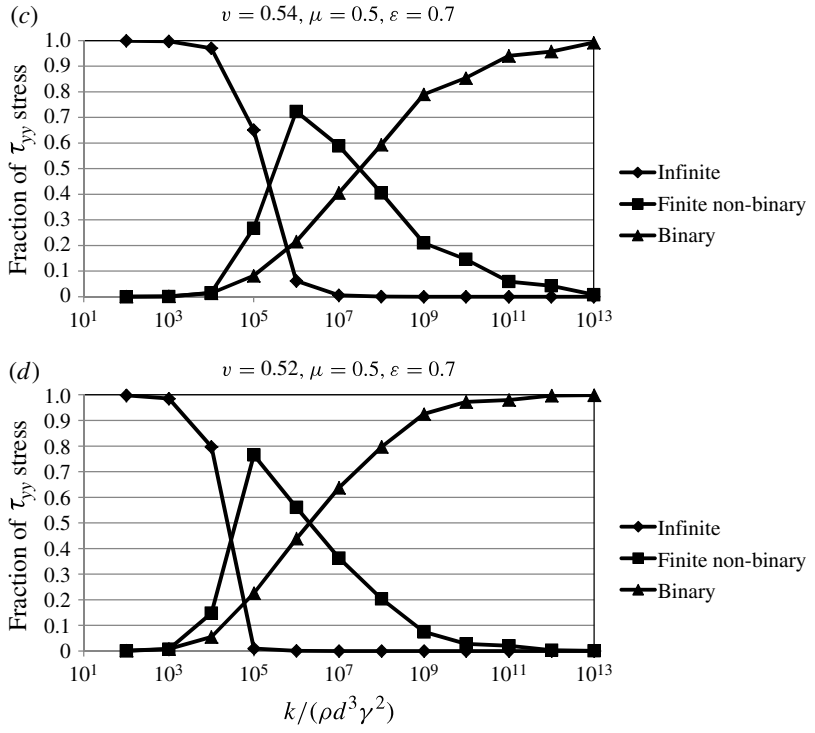

FIGURE 5. The fraction of the τ_{yy} stress supported by infinite, finite non-binary, and binary clusters for four different solid fractions: (*a*) $\nu = 0.58$, (*b*) $\nu = 0.56$, (*c*) $\nu = 0.54$, (*d*) $\nu = 0.52$. Figure 5(*b*) shows a comparison of simulation sizes. For all, $\epsilon = 0.7$ and $\mu = 0.5$.

the clustering process. One role is structural: the larger μ, the more force required to move particles within the cluster and the stronger the clusters. But the other is energetic: the larger μ, the larger the dissipation rate, and in that sense increasing μ has a similar effect to decreasing ϵ.

4. The implications

This work has some surprising implications. Figure 1 indicates that the scaled stress $\tau_{yy}/(\rho d^2\gamma^2)$ is independent of $k^* = k/\rho d^3\gamma^2$ throughout the inertial regime. Suppose one fixes ρ, d, and γ. Then, as long as we remain in the inertial regime, figure 1 tells us that τ_{yy} is fixed. But one can still increase k^* by increasing the interparticle stiffness k. Figures 5–7 then indicate that the system will go from one whose rheology is dominated by infinite clusters to one whose rheology is dominated by binary collisions, with no change in the numerical value of the stress. One goes from a system where internally, momentum is transported by the deformation of interparticle contacts and progresses at the sound speed of the material, to one in which the transport is collisional and rate-limited by the granular temperature.

The confusion is somewhat compounded by figure 8, which shows time traces of the stress for $\nu = 0.54$ as the system transitions from elastic to collisional behaviour with increasing k^*. The first figure for $k^* = 10^2$ shows the characteristics of an elastic system with a series of wide peaks. These peaks form as particles are forced together

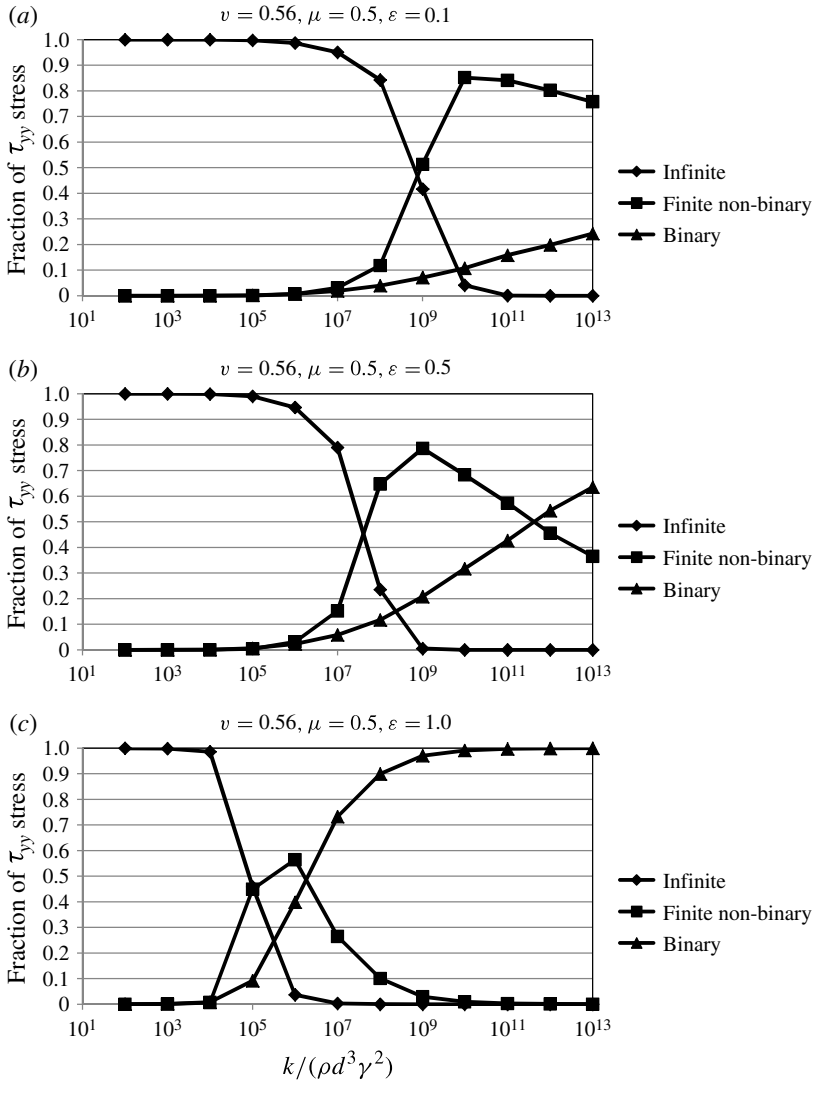

FIGURE 6. The fraction of the τ_{yy} stress supported by infinite, finite non-binary, and binary clusters for three values of the coefficient of restitution ϵ: (*a*) $\epsilon = 0.1$, (*b*) $\epsilon = 0.5$, (*c*) $\epsilon = 1.0$. (The $\epsilon = 0.7$ case can be seen in figure 5*b*.) For all, $\mu = 0.5$ and $\nu = 0.56$.

by the shear flow to form force chains, which are then rotated by the shear until they collapse. As a result the widths of the peaks scale with the shear rate. At the other end is the last plot for $k^* = 10^{13}$ which, according to figure 5(*c*), is rheologically collisional. There the trace is dominated by collisional spikes whose width is determined by the binary collision time, and is thus independent of the shear rate. The transition between the two is quite smooth. One would be hard-pressed looking at the second, $k^* = 10^4$, plot to realize that there has been a transition from elastic to inertial rheology: it is still dominated by the wide peaks reminiscent of elastic behaviour. But then slowly the collisional spikes take over, although there is still some evidence of the wide elastic peaks, even in the collisional $k^* = 10^{13}$ plot.

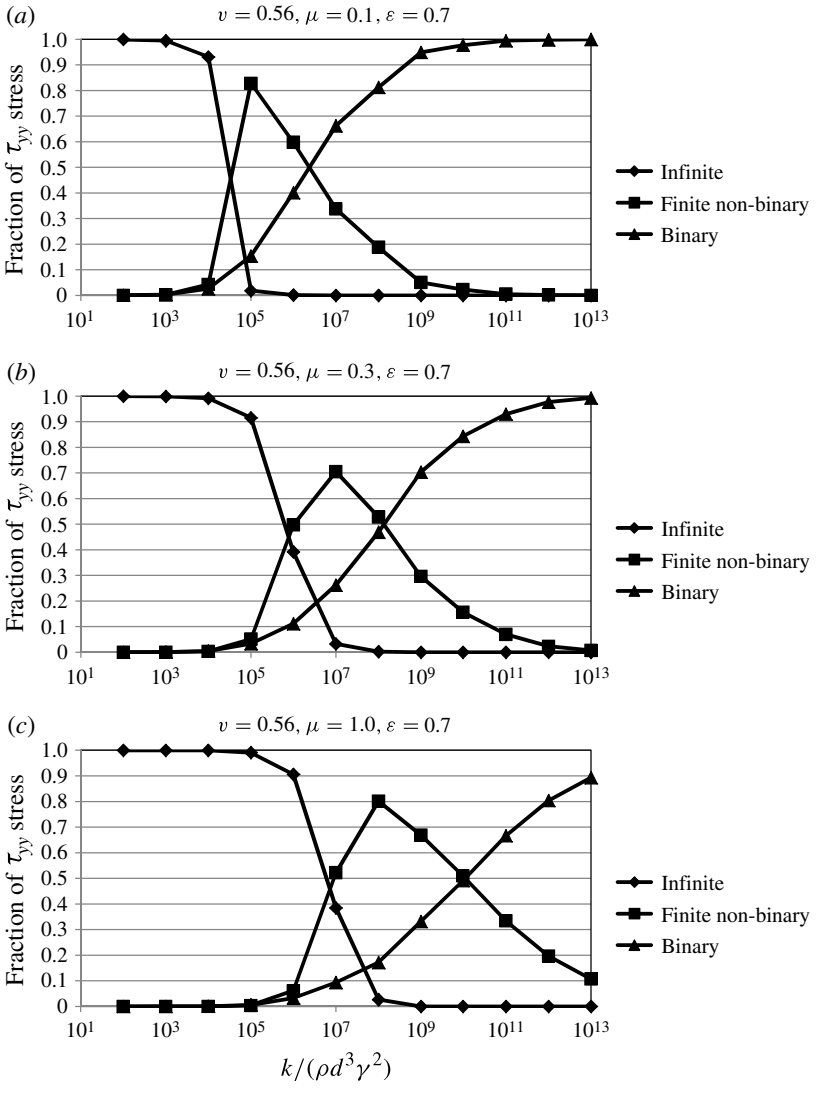

FIGURE 7. The fraction of the τ_{yy} stress supported by infinite, finite non-binary, and binary clusters for three values of the surface friction coefficient μ: (*a*) $\mu = 0.1$, (*b*) $\mu = 0.3$, (*c*) $\mu = 1.0$. (The $\mu = 0.5$ case can be seen in figure 5*b*.) For all, $\epsilon = 0.7$ and $\nu = 0.56$.

This is very troubling to those of us who were taught that the rheology should be a reflection of the micromechanics of the material. The results indicate that it should be possible to analyse the flow for perfectly collisional systems at the rigid particle limit and get an answer that is accurate for systems dominated by infinite clusters (and vice versa). In other words, the physics can be all wrong, yet the answer is all right.

Yet at the same time it is clear that clusters do play a role in the internal momentum transport. Comparing figures 3(*c*) and 5(*b*), one can see that 100 % of the stress is supported by infinite clusters that comprise between only 40 % and 90 % of the particles with a peak around 70 %; in such a case around 30 % of the particles play an insignificant role in generating the stress. And at the other end, it is hard to imagine how, in a thermalized collisional system within which particles are not in contact for

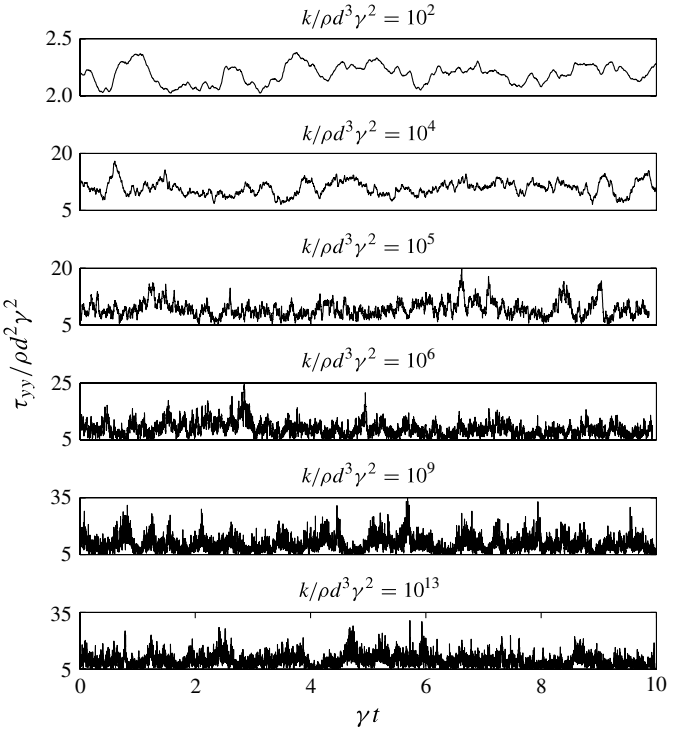

FIGURE 8. Time-dependence of the inertially scaled yy stress, $\tau_{yy}/\rho d^2\gamma^2$, versus time scaled with the shear rate γt, for $\nu = 0.54$. Comparing with figures 1 and 5(*c*), one can see that, rheologically, the top figure, $k^* = k/\rho d^3\gamma^2 = 10^2$, is a purely elastic flow, the second figure, $k^* = 10^4$, is just beyond the transition from elastic to inertial behaviour, and the final figure, $k^* = 10^{13}$, is a purely collisional flow.

longer than a collision time, that all the particles are not involved in generating the stress. Thus the transport processes in infinite clusters must be different from those in a collisional system, but both yield the same stress values.

As of this time, there is no answer to this puzzle. It would be nice if there were some balance between the elastic sound speed and the granular temperature, so that as one transitions from large clusters to collisional behaviour the transport rate remains constant. But it is clear this is not the case. Note that one can interpret $k^* = k/\rho d^3\gamma^2$ as the ratio of the square of the sound speed ($\sim k/\rho\,\mathrm{d}$) to the granular temperature ($\sim d^2\gamma^2$). (The relationship between the granular temperature and $\sim d^2\gamma^2$ can be found in many places, for example Campbell 1989.) Thus, increasing k^* increases the ratio of elastic sound speed to granular temperature so the ratio between the two cannot approach a limiting value. One might think that increasing the sound speed increases the elastic transport rate, but that is at best a small part of the problem here, as increasing the sound speed by increasing k primarily causes the breakdown of clusters and the transition to collisional behaviour, not an increase in elastic transport rates.

Another possibility is that the short lifetime of a cluster limits the elastic transport. Remember that a typical contact time in a cluster is a few binary collision times. As far as a particle is concerned, its cluster must persist for at least the duration of its contacts, so the lifetime of a cluster must be several binary contact times. The binary

collision time is of the order of the time it takes an elastic wave to cross a particle. Thus, a contact time of a few binary collision times indicates that momentum can be transported only a few particle diameters before the cluster disintegrates (however, that only limits the elastic transport – it does not eliminate it entirely – so it is surprising there is still not some effect). One can imagine a situation where a particle collides with a cluster, producing an elastic wave that travels relatively quickly down the cluster until the cluster loses its integrity, after which the momentum is carried relatively slowly away by the granular temperature. On the other hand, in a collision momentum is elastically exchanged over the distance of the single particle diameter between the impacting particle centres. Thus one would still expect an enhancement due to the rapid elastic transport of stress, even if only for several particle diameters.

The other possibility is that there is a rate-limiting bottleneck in the system. For example, if one pictures the system as clusters sitting in a cloud of thermalized particles, then the momentum transported through the cluster must ultimately be carried away through the cloud by the granular temperature. Assuming once again that the elastic transport through the cluster is faster than through the thermal cloud, then the granular temperature becomes the rate-limiting factor. For the overall transport rate to be constant, this picture would indicate that granular temperature should be constant throughout the dense-inertial regime. If the rate-limiting effect is constant, then the stresses can stay constant even though the internal structure is changing. However, one must be careful in defining the granular temperature in systems filled with clusters. (See Campbell 2006*a* for a discussion on what is and what is not granular temperature.) One cannot simply define it as the deviation from the mean velocity, as the particles in a cluster may undergo coordinated motions that may deviate from the mean velocity of the system; but as these coordinated motions do not induce collisions between particles, they do not drive the transport rate and thus it is not technically a granular temperature (or it is, at least, not the granular temperature that appears in kinetic theory models). In fact, in these systems granular temperature can only be unambiguously defined for isolated particles (that is, particles that for the moment, have no contacts with other particles) – and that fits perfectly within the physical model of clusters embedded in a cloud of thermalized particles. Figure 9 shows the isolated particle granular temperature scaled with the shear rate. The results are somewhat interesting. In particular, each set of data shows a peak at the point of transition from elastic to inertial behaviour. This suggests that at this point granular temperature is being generated by the breakdown of force chains. But for most of the inertial range $T/d^2\gamma^2$ is approximately constant. (The one exception is the $\nu = 0.58$ data, but remember, as can be seen in figure 1, this exhibits some transitional behaviour and is not entirely in the inertial regime.) Once again, if one fixes γ and varies k then one can cross much of the range of the plot with a constant granular temperature. This is supportive of the notion that the granular temperature may be the rate-controlling parameter. However, the argument is far from complete.

5. Conclusions

This paper has examined clusters, assemblies of contacting particles, formed in dense-inertial granular flows. These flows behave inertially in the sense that the stresses follow a Bagnold scaling, but internally are not collisional due to the existence of the clusters. The cluster formation is a combination of both elastic and inelastic

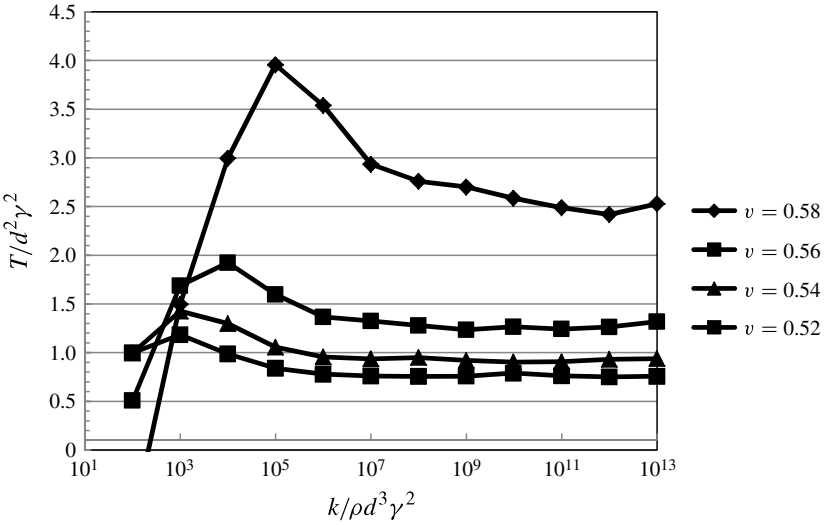

FIGURE 9. Inertially scaled isolated particle granular temperature, $T/d^2\gamma^2$, as a function of the elastic parameter $k/\rho d^3\gamma^2$. The peak in each curve corresponds to the transition from elastic to inertial behaviour.

effects. Their elastic source is apparent as clusters appear at small values of the elastic parameter $k^* = k/\rho d^3\gamma^2$. Small k^* implies small stiffness k or large shear rate γ, and so that the shear rate pushes the particles together quickly relative to the rate at which the elastic forces push them apart, thus forcing cluster formation. In the inelastic sense, the larger the internal dissipation (the smaller the coefficient of restitution), the more likely clusters are to form. Finally, large friction aids cluster formation in two ways. On one hand, the larger the friction, the stronger the cluster. But at the same time larger friction dissipates more energy and further promotes cluster formation.

But there is a most surprising conclusion for this work. At fixed concentration in the dense-inertial regime, the Bagnold scaled stress $\tau/\rho d^2\gamma^2$ does not vary with $k/\rho d^3\gamma^2$. If one fixes ρ, d, and γ, one fixes the stress, but can still move across the range of $k/\rho d^3\gamma^2$ by varying the particle stiffness k. In doing so one moves from a region where 100 % of the stress is supported by infinite clusters (which involve only a fraction of the particles) to one that is entirely collisional without changing the numerical value of the stress. This is of great value to modellers as it allows one to model dense-inertial flows at the rigid particle limit, assuming only collisional interactions and avoiding the difficulty of modelling clusters. (This does not necessarily imply that dense-inertial flows can be modelled using current kinetic theory methods as one must still include surface friction and reasonable dissipation in the model. Also at these concentrations, one would expect stronger correlations between the particle positions and velocities violating the assumptions of statistical randomness inherent to kinetic theories.) But at the same time it is physically troubling, as one expects that the microstructure should have a strong effect on the rheology, while here it apparently does not.

It is far from clear why the clusters have so little effect on the rheology. One possibility is that the clusters are so short-lived that they have little opportunity to enhance the transport rates. But the most promising prospect is that the granular temperature, which transports momentum both between clusters and away from broken

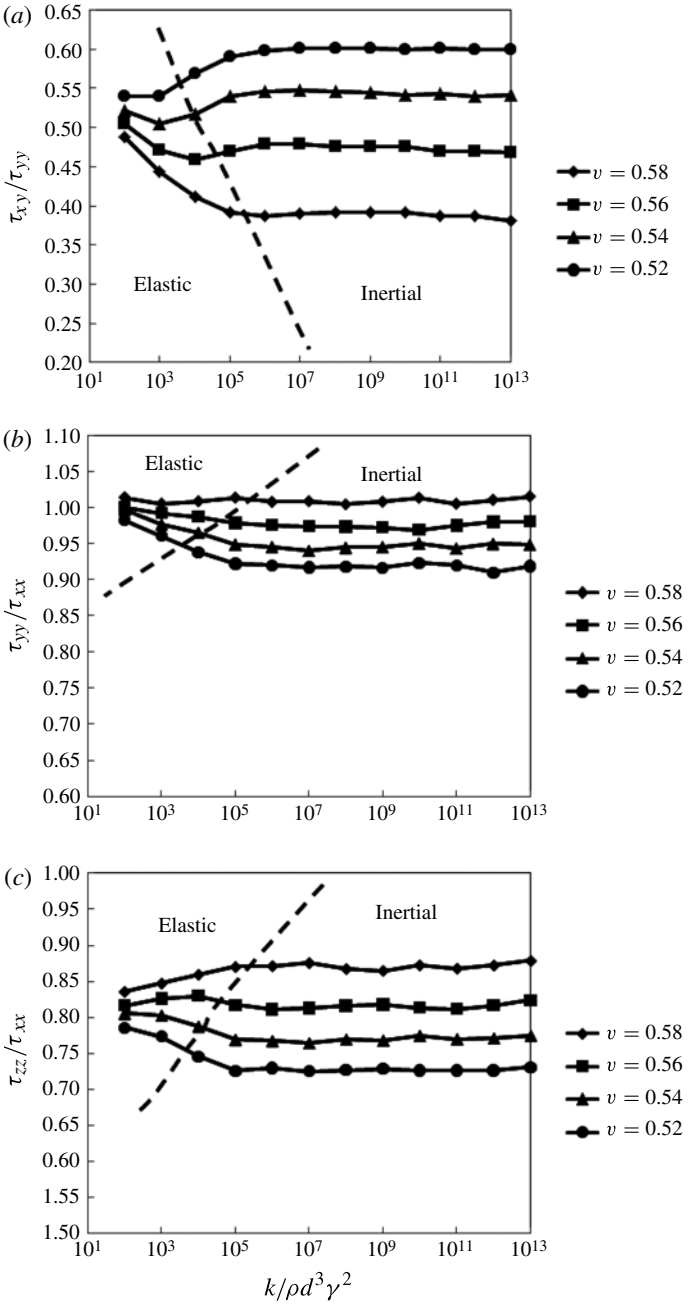

FIGURE 10. The stress ratios for the data shown in figure 1. (*a*) The apparent friction coefficient τ_{xy}/τ_{yy} and the normal stress ratios, (*b*) τ_{yy}/τ_{xx} and (*c*) τ_{zz}/τ_{xx}. Here $\epsilon = 0.7$, $\mu = 0.5$. The dashed lines indicate roughly the transition from elastic to inertial flow.

clusters, is acting as a rate-limiting bottleneck. This best indication of this is that under the same conditions of fixed ρ, d and γ, the granular temperature is nearly constant over the full range of k^*. But piecing together this puzzle will require more research.

This work was supported by the National Science Foundation under grant CBET-0828514, for which the author is truly grateful. Many thanks to Carl Wassgren and Vincent Hoon for allowing access to their Particlevis software.

Supplementary material is available at journals.cambridge.org/flm.

Appendix

A referee asked that the stress ratio data corresponding to figure 1 be included in the paper. The author feels that to add these plots to figure 1 would distract from the narrative of the paper, but is happy to include the figures: see figure 10. Note that for the normal stress ratios, figure 10(*b*,*c*), τ_{xx} is used in the denominator because it is usually the largest of the normal stress components. However, there are cases in figure 10(*b*) for $\nu = 0.58$ where τ_{yy} slightly exceeds τ_{xx}.

REFERENCES

BAGNOLD, R. A. 1954 Experiments on a gravity-free dispersion of large solid particles in a Newtonian fluid under shear. *Proc. R. Soc. Lond.* A **225**, 49–63.

CAMPBELL, C. S. 1989 The stress tensor for simple shear flows of a granular material. *J. Fluid Mech.* **203**, 449–473.

CAMPBELL, C. S. 2002 Granular shear flows at the elastic limit. *J. Fluid Mech.* **465**, 261–291.

CAMPBELL, C. S. 2003 A problem related to the stability of force chains. *Granular Matt.* **5**, 129–134.

CAMPBELL, C. S. 2005 Stress-controlled elastic granular shear flows. *J. Fluid Mech.* **539**, 273–297.

CAMPBELL, C. S 2006*a* Granular flows: an overview. *Powder Technol.* **162**, 208–229.

CAMPBELL, C. S. 2006*b* Computer simulation of powder flows. In *Powder Technology Handbook* (ed. K. Gotoh, H. Masuda & K. Higashitani). 3rd edn. pp. 737–748. Taylor and Francis.

CUNDALL, P. A. & STRACK, O. D. L. 1979 A discrete numerical model for granular assemblies. *Geotechnique* **29**, 47–65.

DA CRUZ, F., EMAM, S., PROCHNOW, M., ROUX, J. N. & CHEVOIR, F. 2005 Rheophysics of dense granular materials: discrete simulation of plane shear flows. *Phys. Rev.* E **72**, 021309.

FORTERRE, Y. & POULIQUEN, O. 2006 Flows of dense granular media. *Annu. Rev. Fluid Mech.* **40**, 1–24.

MIDI, G. D. R. 2004 On dense granular flows. *Eur. Phys. J.* E **14**, 341–365.

HOPKINS, M. A. & LOUGE, M. Y. 1991 Inelastic microstructure in rapid granular flows of smooth disks. *Phys. Fluids* A **3**, 47–57.

JANSSEN, H. A. 1895 Versuche über Getreidedruck in Silozellen. *Zeitschrift des Vereines deutscher Ingenieure* **39**, 1045–1049.

JOP, P., FORTERRE, Y. & POULIQUEN, O. 2006 A constitutive law for dense granular flows. *Nature* **441**, 727–730.

LEES, A. W. & EDWARDS, S. F. 1972 The computer study of transport processes under extreme conditions. *J. Phys. C: Solid State Phys.* **5**, 1921–1929.

LOIS, G., LEMAITRE, A. & CARLSON, J. M. 2007*a* Spatial force correlations in granular shear flow. Part I. Numerical evidence. *Phys. Rev.* E **76**, 021302.

LOIS, G., LEMAITRE, A. & CARLSON, J. M. 2007*b* Spatial force correlations in granular shear flow. Part II. Theoretical implications. *Phys. Rev.* E **76**, 021303.

NAKAGAWA, M., ALTOBELLI, S. A., CAPRIHAN, A., FUKUSHIMA, E. & JEONG, E.-K. 1993 Noninvasive measurement of granular flows by magnetic-resonance imaging. *Exp. Fluids* **16**, 54–60.

POULIQUEN, O., CASSAR, C., JOP, P., FORTERRE, Y. & NICOLAS, M. 2006 Flow of dense granular material: towards simple constitutive laws. *J. Statist. Mech.: Theory and Experiment* **P07020**, 1–14.

WASSGREN, C. & SARKAR, A. 2007 Visualization of particle-based computer data, http://pharmahub.org/resources/4.